

SUPPORTING INFORMATION

for

MOLECULAR RECOGNITION AND SOLVATOMORPHISM IN A CYCLIC PEPTOID. FORMATION OF A STABLE 1D POROUS FRAMEWORK.

Eleonora Macedi,^a Alessandra Meli,^a Francesco De Riccardis,^a Patrizia Rossi,^b Vincent J. Smith,^c Leonard J. Barbour,^c Irene Izzo^{a,} and Consiglia Tedesco^{a,*}*

^aDepartment of Chemistry and Biology "A. Zambelli", University of Salerno, Via Giovanni Paolo II 132, 84084 Fisciano (SA), Italy;

^bDepartment of Industrial Engineering, University of Florence, via S. Marta 3, I-50139 Florence, Italy;

^cDepartment of Chemistry and Polymer Science, University of Stellenbosch, Private Bag X1, 7602 Matieland, Stellenbosch, South Africa.

Corresponding author; email: ctedesco@unisa.it, iizzo@unisa.it

INDEX

List of Abbreviations	S2
1 Synthesis and crystallization	S3
1.1 Crystal forms 1C and 1D	
1.2 Crystal forms 1E and 1F	
2 Single crystal X-ray diffraction	S4
3 Structural analysis	S10
3.1 Superimposition between peptoid backbones	
3.2 Rectangular shape of the macrocycles	
3.3 Side chains orientation	
4 Packing analysis	S12
4.1 Hirshfeld surface analysis	
4.2 CLP-Pixel calculations	
5 Gas phase optimizations and energies	S17
6 Thermal analysis	S17
6.1 DSC	
6.2 TGA	
7 Variable temperature X-ray Diffraction	S20
8 Reversibility tests	S22
References	S23

LIST OF ABBREVIATIONS

DSC differential scanning calorimetry

Nme *N*-(methoxyethyl)glycine

Npa *N*-(propargyl)glycine

TGA thermogravimetric analysis

1. SYNTHESIS AND CRYSTALLIZATION

1.1 Crystal forms 1C and 1D

Compound **1** was synthesized as previously described.¹

Form 1C. 3.5 mg of compound **1** were dissolved in 600 μL hot acetonitrile, then 400 μL water were added. Form **1C** crystallized by slow evaporation, obtaining transparent plate-like crystals suitable for laboratory X-ray diffraction studies (Figure S1a).

Form 1D. 4.0 mg of compound **1** were dissolved in 600 μL hot acetonitrile, then 200 μL methanol were added. Form **1D** crystallized by slow evaporation, obtaining transparent plate-like crystals suitable for laboratory X-ray diffraction studies (Figure S1b).

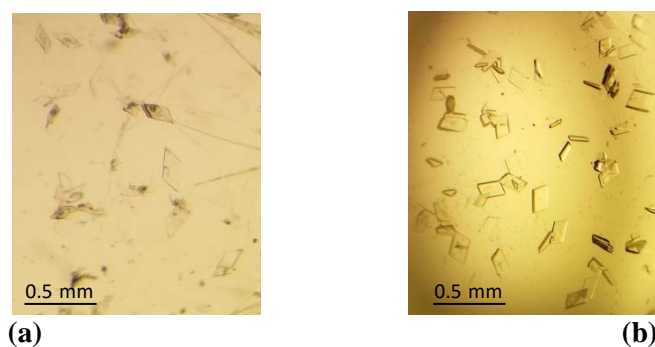


Figure S1. Crystals of (a) **1C** and (b) **1D**.

1.2. Crystal forms 1E and 1F

Form 1E. Crystals of form **1E** were obtained from crystal form **1D** by removing the crystals from the mother liquor and exposing the crystals to ambient humidity (Figure S2).

Form 1F. A crystal of the guest-free form **1F** was obtained from crystal form **1D** by an *in situ* variable temperature single crystal X-ray diffraction analysis. A fresh crystal of **1D** was glued on a glass fiber and analyzed at 100 K, 323 K, 368 K, 393 K and back to 100 K using a nitrogen gas hot blower.

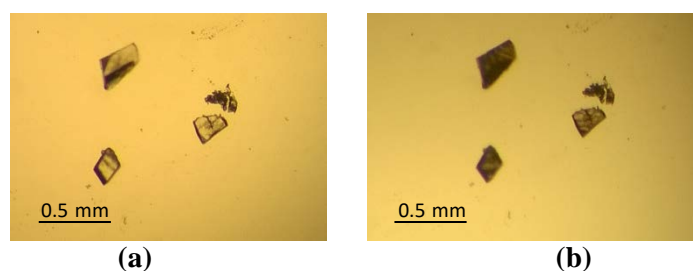


Figure S2. (a) Crystals of form **1D** (left); (b) the same crystals after 10 minutes exposure to air transformed into crystal form **1E**.

2. SINGLE CRYSTAL X-RAY DIFFRACTION

A crystal of form **1C** (0.45 x 0.27 x 0.051 mm) suitable for laboratory X-ray diffraction was selected and mounted on a MiTeGen microloopTM with Paratone® N. Data collection was performed at 296 K with a Rigaku AFC7S diffractometer equipped with a Mercury² CCD detector using graphite monochromated MoK α radiation ($\lambda = 0.71073 \text{ \AA}$). Data reduction was performed with the crystallographic package CrystalClear.² Data were corrected for Lorentz, polarization and absorption.

A crystal of form **1D** (0.27 x 0.24 x 0.10 mm) suitable for laboratory X-ray diffraction was selected and mounted on a MiTeGen microloopTM with Paratone® N. Data collection was performed at 100 K with a Rigaku AFC7S diffractometer equipped with a Mercury² CCD detector using graphite monochromated MoK α radiation ($\lambda = 0.71073 \text{ \AA}$). Data reduction was performed with the crystallographic package CrystalClear.² Data were corrected for Lorentz, polarization and absorption.

A crystal of form **1E** (0.39 x 0.33 x 0.08 mm) obtained by exposing a crystal of form **1D** to ambient humidity was mounted on a MiTeGen microloopTM with Paratone® N. Diffraction data were collected at 100 K on a Bruker DUO Quasar diffractometer equipped with an APEX-II CCD area-detector and an Oxford Cryosystems Cryostream 700Plus cryostream for temperature control. The radiation was produced from an Incoatec I μ S microsource fitted with a multilayer monochromator (MoK α , $\lambda = 0.71073 \text{ \AA}$). Data reduction was performed with the crystallographic package APEX.³

A crystal of form **1F** (0.35 x 0.35 x 0.15 mm) obtained as described above was measured at 100 K by means of an Oxford Diffraction Excalibur diffractometer using Mo K α radiation ($\lambda = 0.71073 \text{ \AA}$). Data collection was performed with the program CrysAlis CCD.⁴ Data reduction was carried out with the program CrysAlis RED (CrysAlis RED, 2006).⁵ Finally, absorption correction was performed with the program ABSPACK in CrysAlis RED.⁵

The structures were solved by direct methods using the program SIR2014⁶ and refined by means of full matrix least-squares based on F^2 using the program SHELXL.⁷

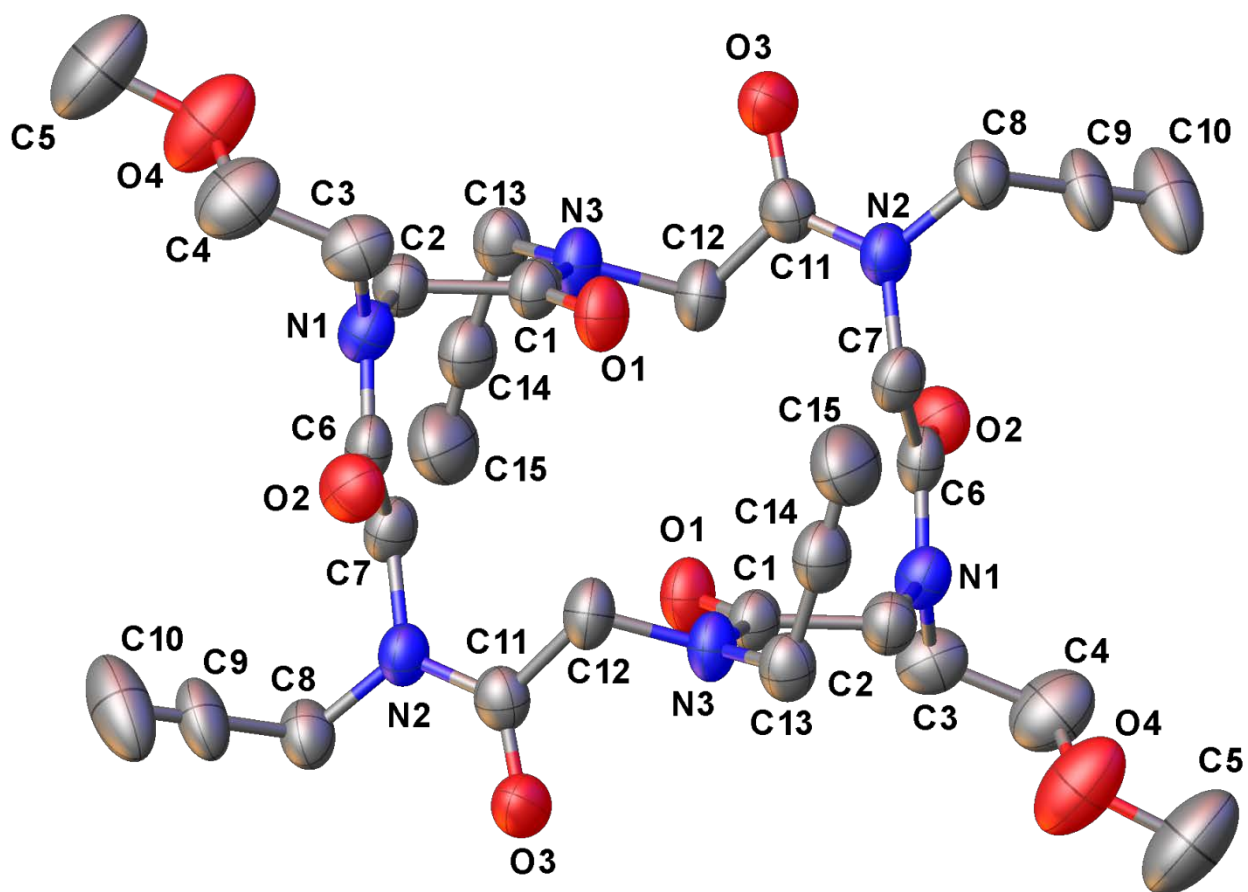
OLEX2⁸ and X-seed⁹ were used as GUI. X-ray molecular structures (ORTEP) were drawn by OLEX2.⁸ Crystal structures were drawn using Mercury (v3.8).¹⁰

For all compounds, non-hydrogen atoms were refined anisotropically.

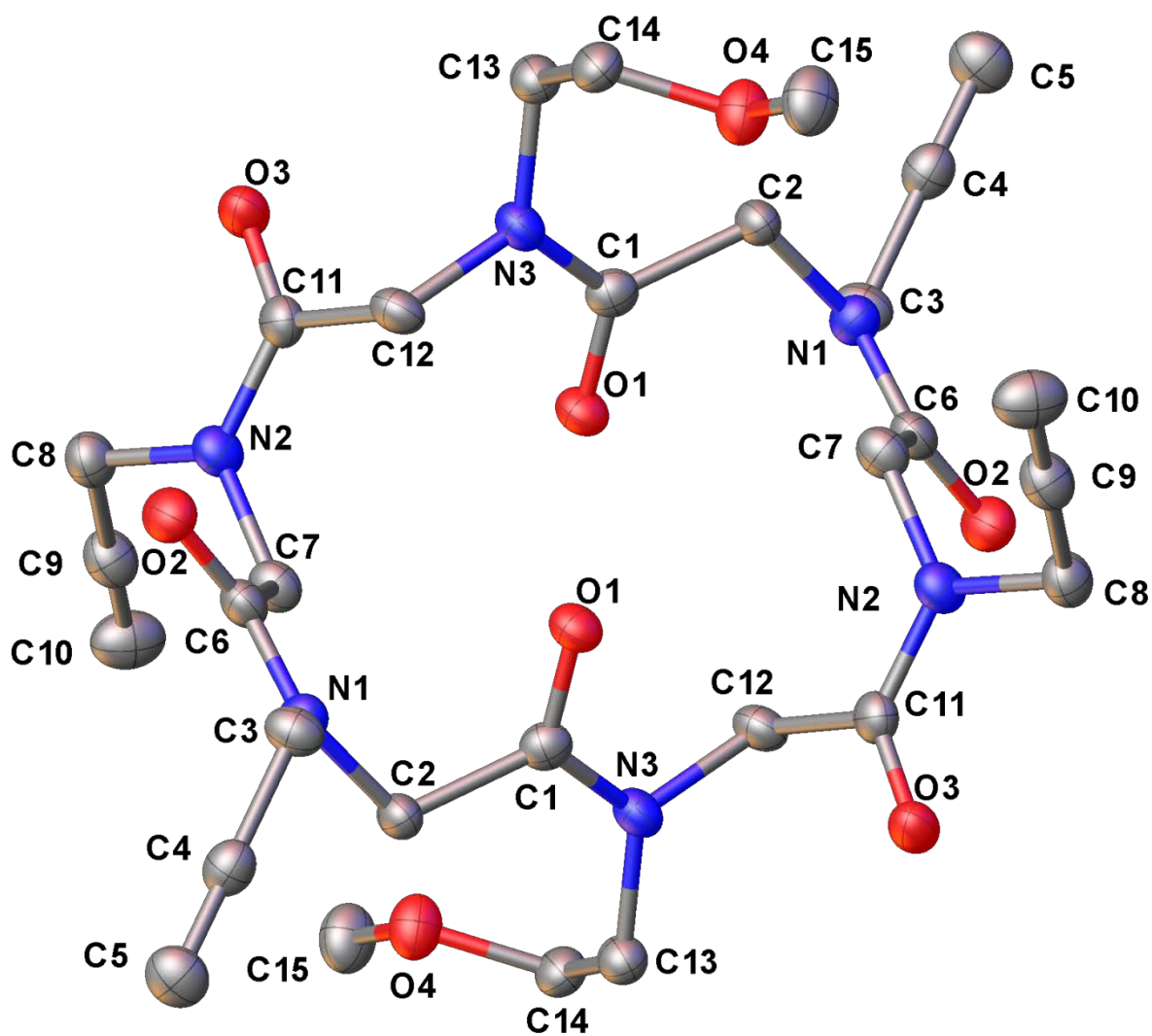
Hydrogen atoms were positioned geometrically and included in structure factors calculations but not refined. In form **1D** the methanol hydroxyl hydrogen atom was located in the Fourier difference map but not refined. In form **1E** the water hydrogen atom hydrogen bonded to the carbonyl atom

O2 was located in the Fourier map and used to define the initial orientation of the water molecule, then the water molecule was refined as a rigid group. The occupancy of the water molecule was also refined to a final value of 0.581(7).

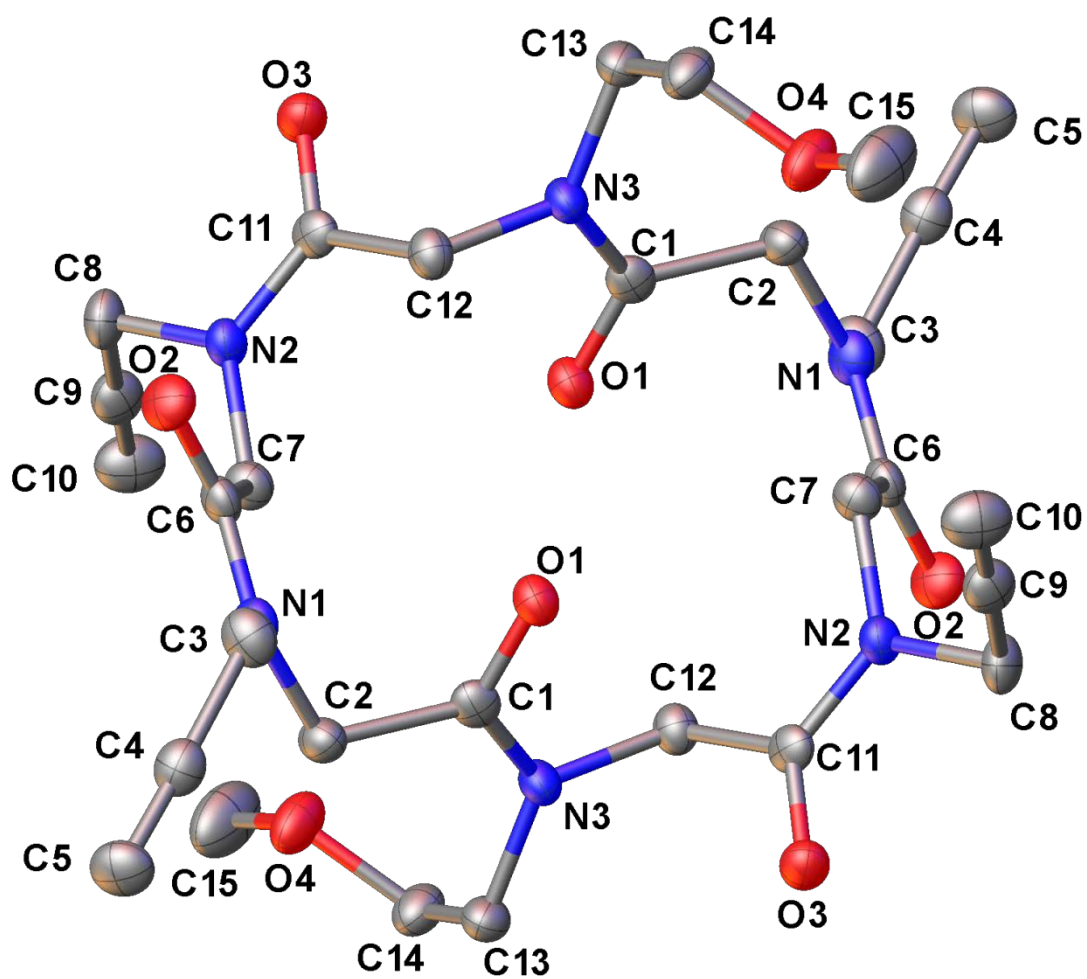
Refinement details are summarized in Table S1 for crystal forms **1C**, **1D**, **1E** and **1F**. ORTEP diagrams are reported in Figure S3.



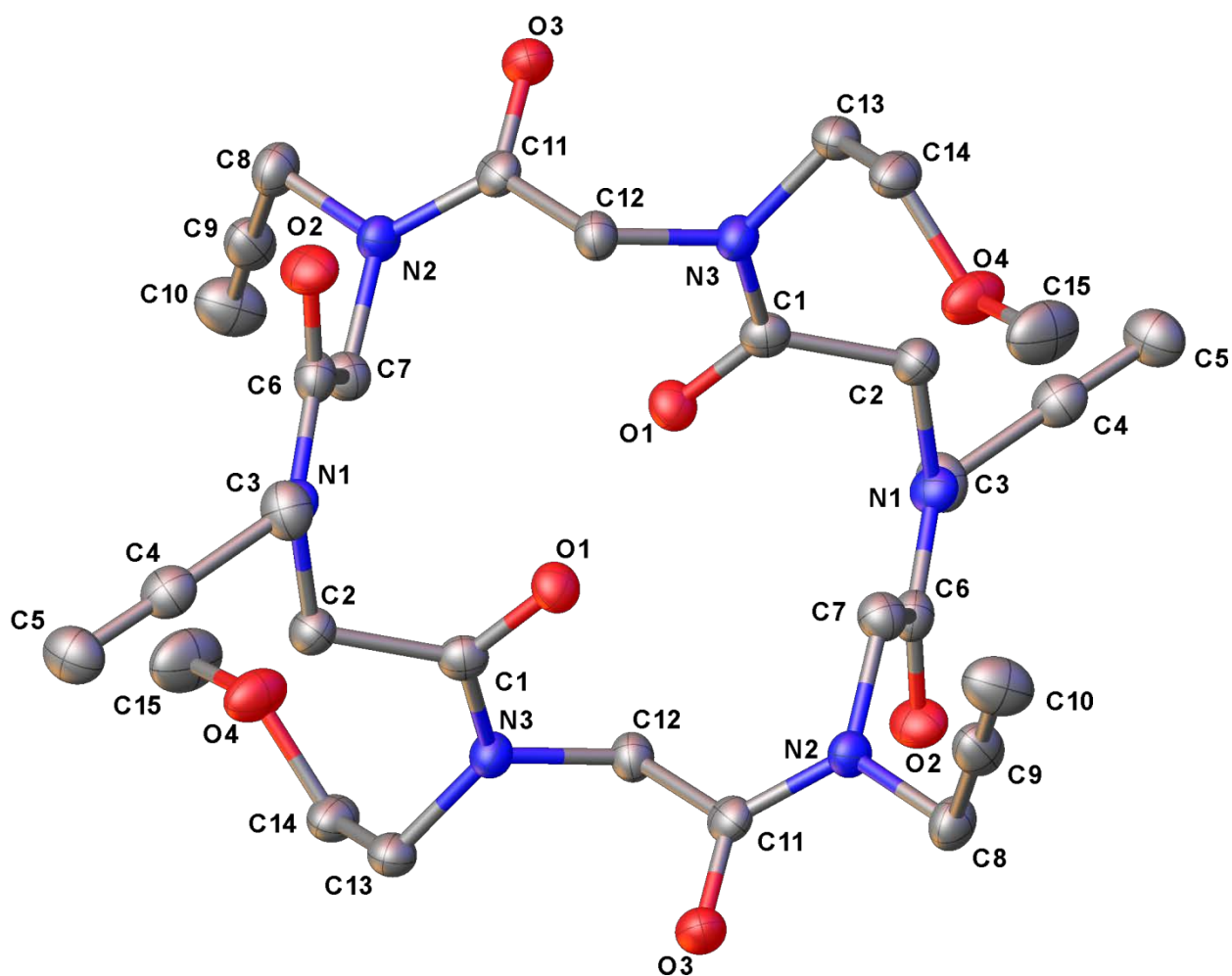
(a) ORTEP diagram for crystal form **1C**.



(b) ORTEP diagram for crystal form **1D**.



(c) ORTEP diagram for crystal form **1E**.



(d) ORTEP diagram for crystal form **1F**.

Figure S3. ORTEP diagrams for the cycloheptimide rings in crystal forms (a) **1C**, (b) **1D**, (c) **1E**, (d) **1F**. Ellipsoids are drawn at 50% probability level. All rings lie about inversion centres and the symmetry-operators between inversion-related atoms are: **1C** $(-x, -y, 1-z)$, **1D** $(-x, 1-y, 1-z)$, **1E** and **1F** $(1-x, 1-y, 1-z)$.

3. STRUCTURAL ANALYSIS

3.1 Superimposition between peptoid backbones

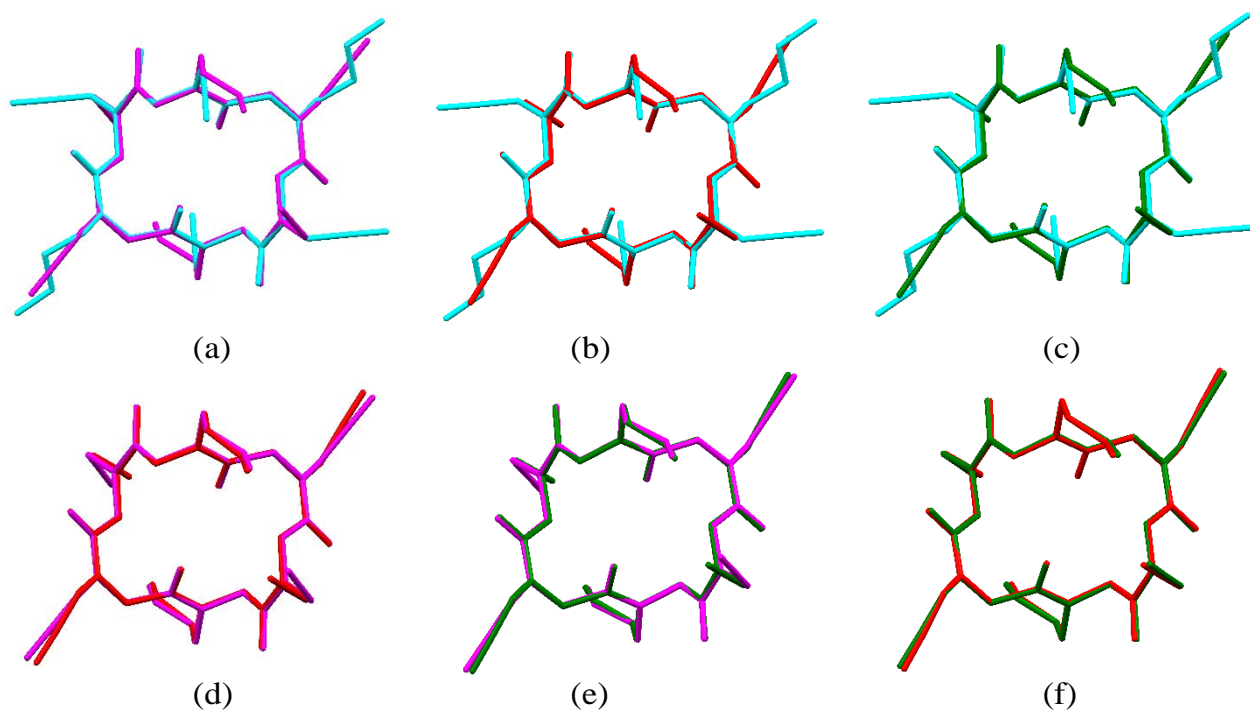


Figure S4. Peptoid backbone overlay between crystal forms: a) **1C** and **1D**, rmsd 0.0622 Å; b) **1C** and **1E**, rmsd 0.0953 Å; c) **1C** and **1F**, rmsd 0.0975 Å; d) **1D** and **1E**, rmsd 0.0462 Å; e) **1D** and **1F**, rmsd 0.0443 Å; f) **1E** and **1F**, rmsd 0.0205 Å. Form **1C**: cyan; form **1D**: magenta; form **1E**: green; form **1F**: red.

3.2 Rectangular shape of the macrocycles

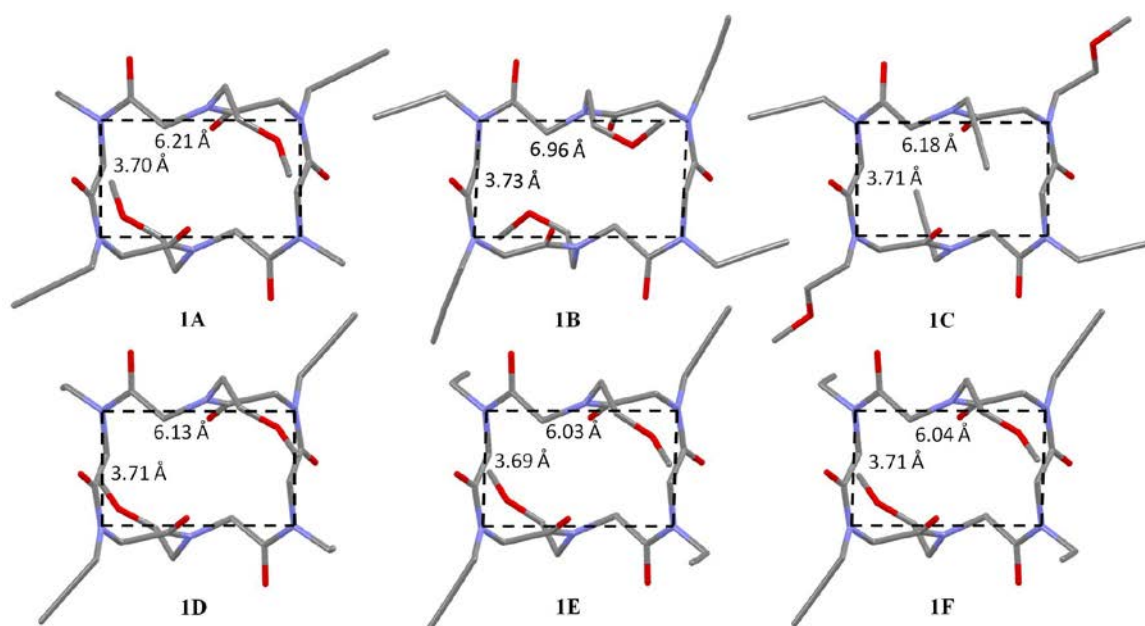


Figure S5. Rectangular shape of the peptoid backbone in crystal forms **1A**, **1B** (type **II** molecule), **1C**, **1D**, **1E** and **1F**. Four *cis* amide bonds reside at each corner, *trans* amide bonds are located on two opposite sides. The values of length and width (Å) are reported.

3.3 Side chains orientation

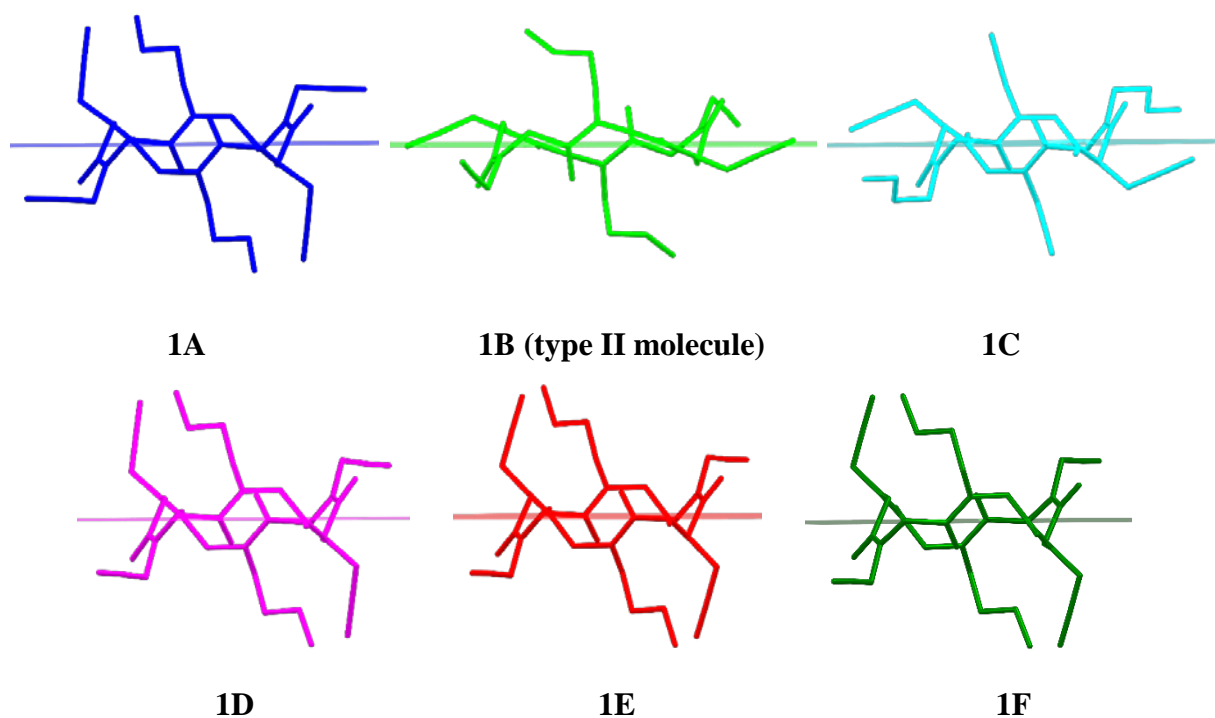


Figure S6. Orientation of the side chains with respect to the macrocycle plane in crystal forms **1A**, **1B** (type **II** molecule), **1C**, **1D**, **1E** and **1F**.

4. PACKING ANALYSIS

4.1 Hirshfeld surface analysis

Hirshfeld surface analysis and related fingerprint plots have been performed with Crystal Explorer 3.1.¹¹

The Hirshfeld surface arises from the partitioning of the electron density of a crystal into molecular fragments.¹² It provides maximum proximity of neighbouring molecular volumes without volumes overlapping.¹³

d_i is the distance from the surface to the nearest atom interior to the surface. d_e is the distance from the surface to the nearest atom exterior to the surface. d_{norm} is a normalized distance, which takes into account the relative atom sizes:¹⁴

$$d_{\text{norm}} = \frac{d_i - r_i^{\text{vdW}}}{r_i^{\text{vdW}}} + \frac{d_e - r_e^{\text{vdW}}}{r_e^{\text{vdW}}}$$

where r^{vdW} is the van der Waals (vdW) radius of the appropriate atom internal or external to the surface.

Relative contributions to the Hirshfeld surface area of particular types of intermolecular contacts are determined by summing the area corresponding to close contacts between specific types of atoms.¹⁴

The lengths of X–H bonds are normalized using standard X–H distances from Allen *et al.*¹⁵ Thus, reported X–H distances and X···H contacts are not equal to those calculated from the original cif files.

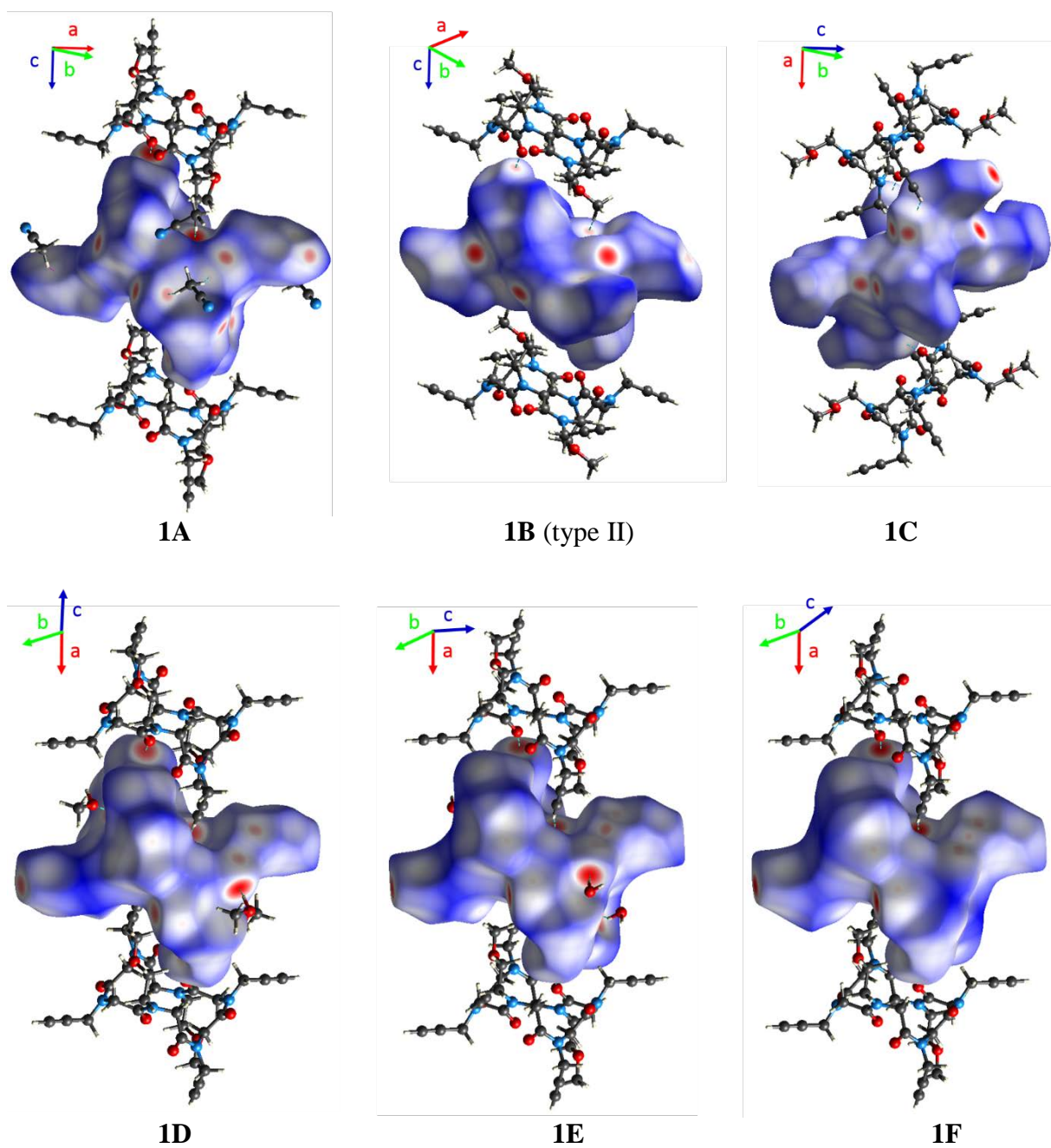
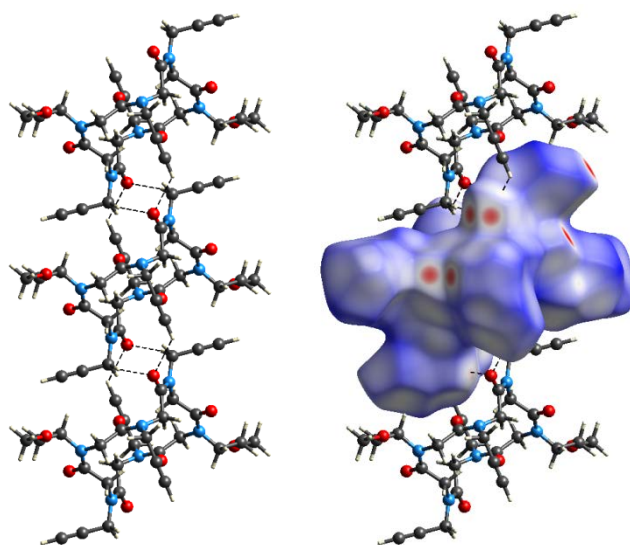
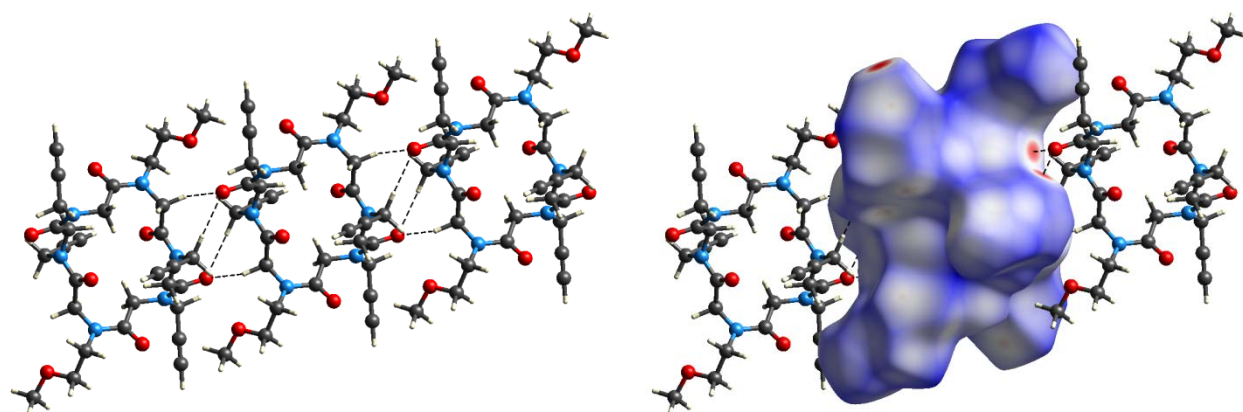


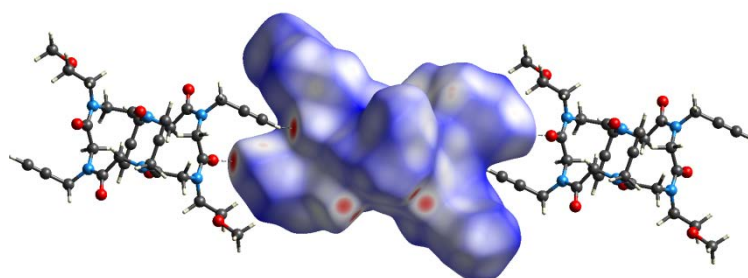
Figure S7. Hirshfeld surfaces of cyclopeptoid molecules in crystal forms a) **1A**, b) **1B** type II, c) **1C**, d) **1D**, e) **1E** and f) **1F**. C=O...H-C hydrogen bonds are depicted respectively as dotted lines.



Motif I

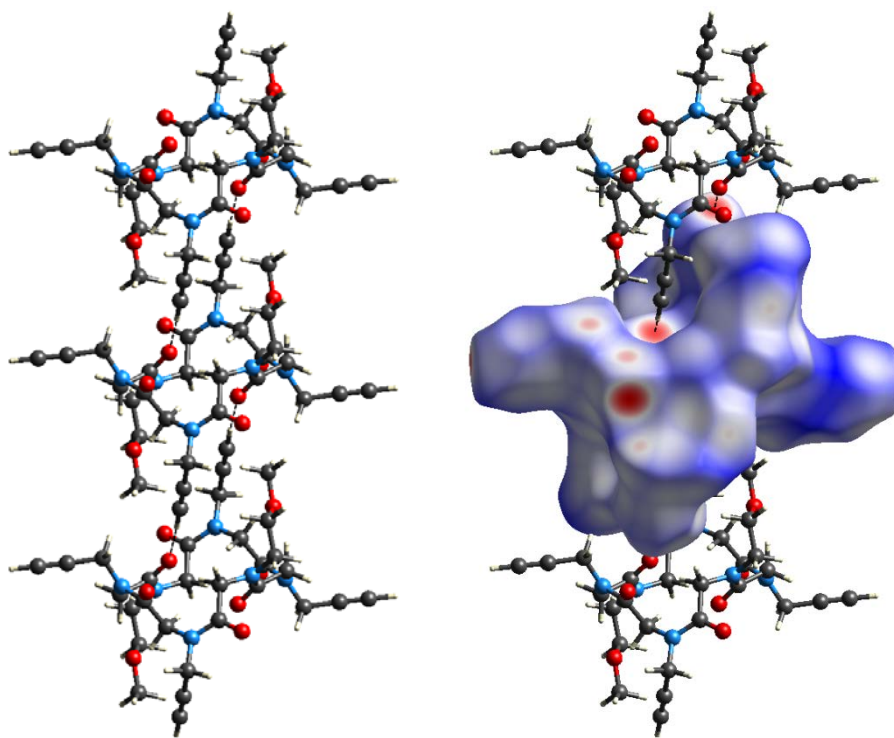


Motif II

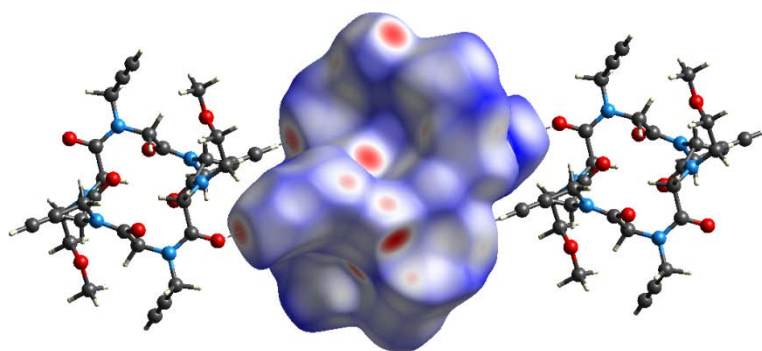
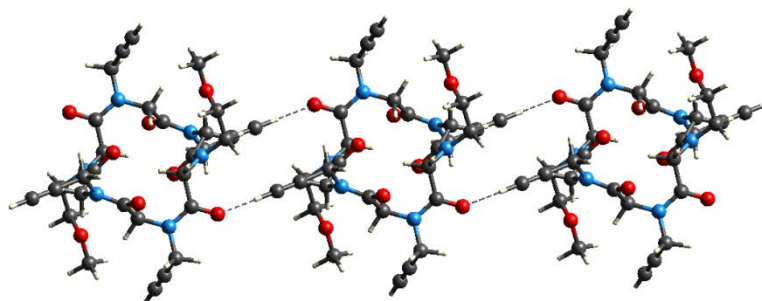


Motif III

Figure S8. Hirshfeld surface and assembly motifs in crystal form **1C** (see also Table S1).



Motif I



Motif II

Figure S9. Hirshfeld surface and assembly motifs in crystal form **1D** (see also Table S2).

4.2 CLP-Pixel calculations

The lattice energy of all the crystal forms was calculated using the CLP-Pixel package.¹⁶ The total lattice energy is partitioned into its coulombic, polarization, dispersion and repulsion contributions (Tables S2-S3). In CLP-Pixel, the coulombic terms are handled by Coulomb's law, while the polarization terms are calculated in the linear dipole approximation, with the incoming electric field acting on local polarizabilities and generating a dipole with its associated dipole separation energy; dispersion terms are simulated in London's inverse sixth power approximation, involving ionization potentials and polarizabilities; repulsion is presented as a modulated function of wavefunction overlap. Selected motifs in the crystal packing of both crystal forms **1C** and **1D** were analyzed by means of their interaction energies (Tables S2-S3).

In both crystal forms the centre of gravity of the cycloheptoid molecules is located on a crystallographic inversion centre. Therefore, to consider a whole cycloheptoid molecule in the CLP calculations, the space group symmetry was lowered to *P1* for crystal forms **1C** and **1D**. The lengths of X–H bonds are normalized using standard X–H distances from Allen *et al.*¹⁵ Thus, the values given throughout the discussion in the main text and in this Supporting information refer to the re-calculated structures.

Table S1. List of intermolecular distances (Å), angles (°) and interaction energies (kJ/mol) in crystal form **1C** as calculated by CLP-PIXEL.

Motif	D-H...A	D...A dist.	H...A dist.	<D-H...A angle	Symm. Op.	Centre of mass dist.	E_{coul}	E_{pol}	E_{disp}	E_{rep}	E_{tot}
I	C13-H13B...O3	3.387(1)	2.31	179	$x, -1+y, z$ $x, 1+y, z$	9.094(2)	-60.3	-26.6	-70.8	63.7	-93.9
II	C8-H8A...O3	3.596(1)	2.56	160	$-1+x, y, z$	8.814(3)	-45.1	-15.9	-63.2	52.8	-71.4
	C15-H15...O3	3.348(1)	2.56	129	$1+x, y, z$						
III	C10-H10...O2	3.174(1)	2.14	159	$-1+x, y, 1+z$ $1+x, y, -1+z$	13.785(4)	-39.5	-12.4	-22.5	34.8	-39.6
IV	H15-C15...H2A-C2	3.476	2.76	71	$-1+x, 1+y, z$ $1+x, 1-y, z$	9.802(2)	-14.3	-6.3	-39.7	22.0	-38.3

Table S2. List of intermolecular distances (Å), angles (°) and interaction energies (kJ/mol) in crystal form **1D** as calculated by CLP-PIXEL.

Motif	D-H...A	D...A dist.	H...A dist.	<D-H...A angle	Symm. Op.	Centre of mass dist.	E_{coul}	E_{pol}	E_{disp}	E_{rep}	E_{tot}
I Cp-Cp	C10-H10...O1	3.107(1)	2.03	178	$-1+x, y, z$ $1+x, y, z$	8.501(1)	-76.5	-31.4	-92.1	105.4	-94.6
II Cp-Cp	C5-H5...O3	3.233(1)	2.17	169	$x, -1+y, 1+z$ $x, 1+y, -1+z$	11.901(2)	-43.0	-13.2	-26.7	34.3	-48.7
III Cp-MeOH	O15-H15...O2	2.789(1)	1.793	173	x, y, z	6.530(1)	-55.5	-22.0	-24.5	64.6	-37.5
IV Cp-MeOH	C7-H7B...O15	3.163(1)	2.188	149	$1+x, 1-y, z$	6.092(1)	-20.3	-9.2	-24.8	31.3	-22.9

5. GAS-PHASE OPTIMIZATIONS AND ENERGIES

Molecular energies were determined by gas-phase geometry optimizations carried out with density functional theory including dispersion corrections (DFT-d) at the B97-D3/ccpVTZ level of theory using the Gaussian09 package.¹⁷ The functional B97-D3 includes van der Waals corrections as derived by Grimme and co-workers.¹⁸

6. THERMAL ANALYSES

6.1 DSC

DSC measurements were performed on a TA DSC-Q20 instrument.

Single crystals of forms **1C** (up to 1.6000 mg) and **1D** (up to 1.1000 mg) were removed from the mother liquor, quickly dried on filter paper to remove surface solvent and placed in DSC aluminium pinhole pans and heated at a rate of 2 °C/min under a purified N₂ flow (50 mL/min) from 20 °C to 300 °C.

DSC analysis on single crystals of form **1C** shows the stability of the sample up to 190 °C, then it decomposes (Figure S10).

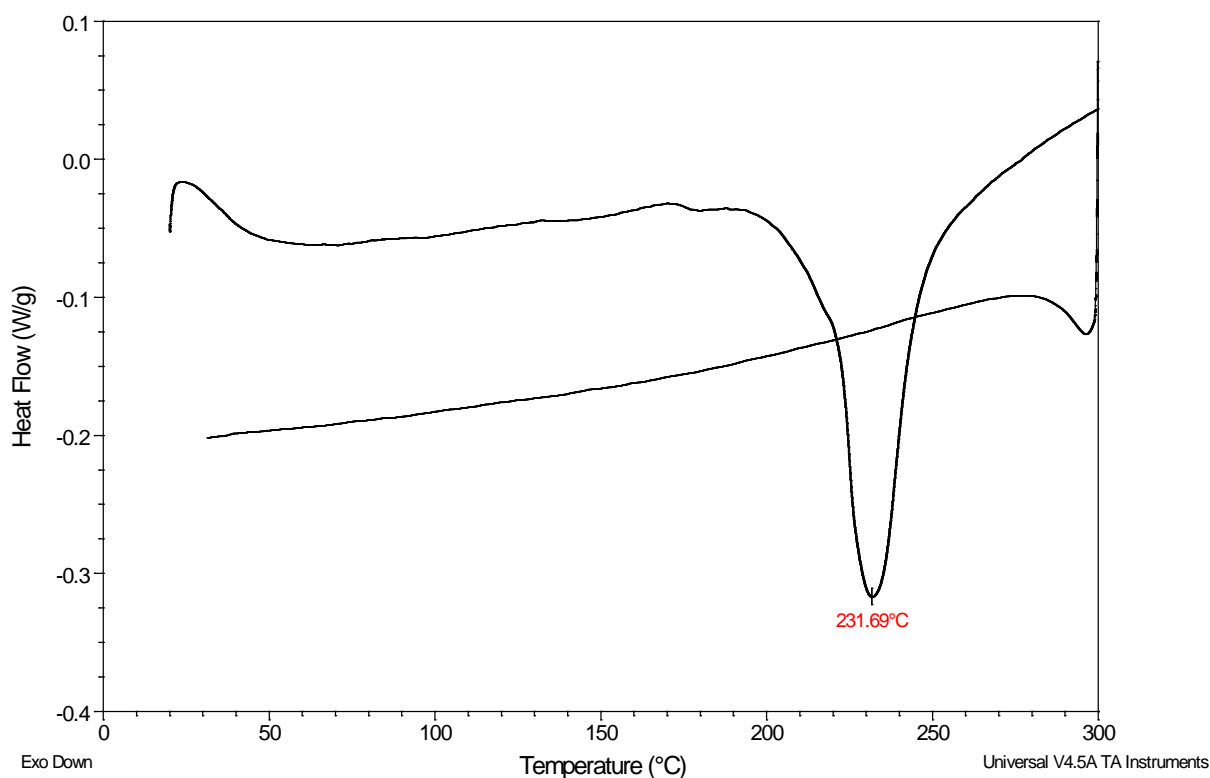


Figure S10. DSC analysis on crystals of form **1C**.

DSC analysis on single crystals of form **1D** shows the release of methanol molecules between 30 °C and 90 °C, followed by a complex behavior determined by a couple of two closely occurring endothermic and exothermic events, starting respectively at 184 °C and 215 °C, with an overall enthalpy change of *ca.* 7.7 and 5.4 J g⁻¹, respectively (4.7 and 3.3 kJ mol⁻¹). Finally decomposition occurs (T > 230 °C) (Figure S11).

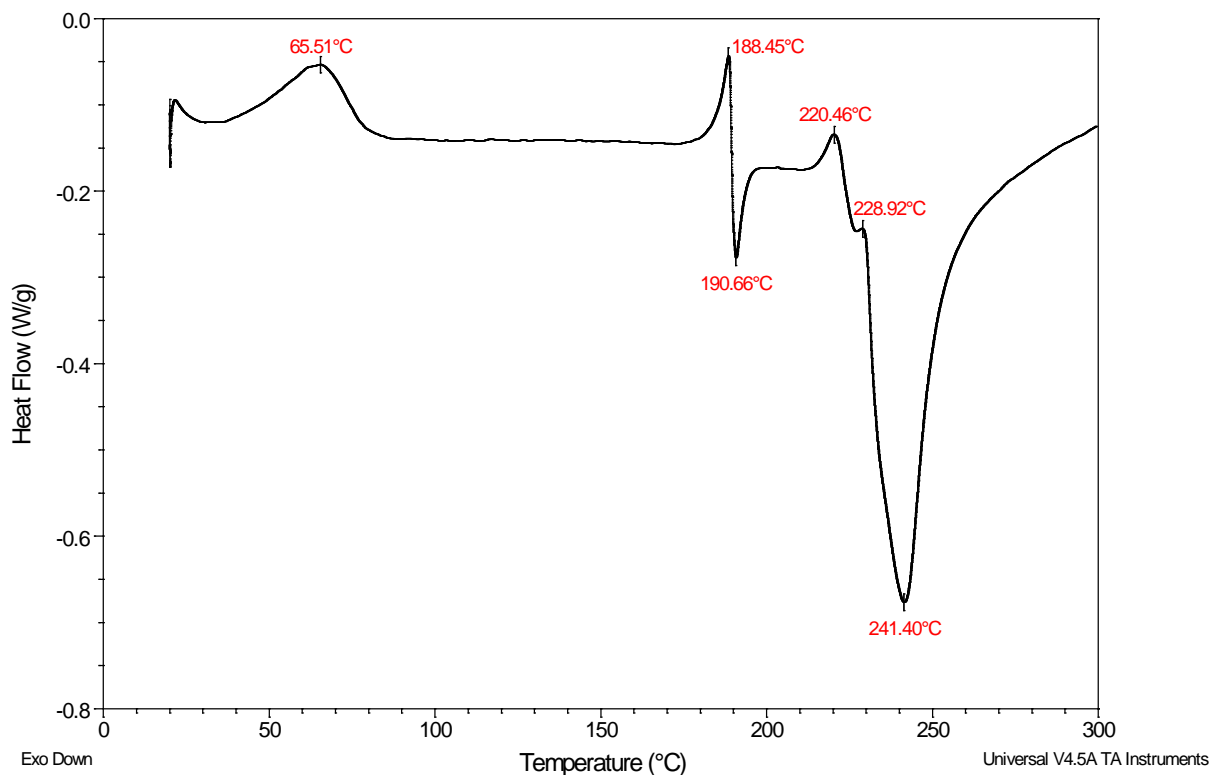


Figure S11. DSC analysis on crystals of form **1D**. Methanol molecules are released in the temperature range from 30 °C to 90 °C.

6.2 TGA

TGA measurements were performed on a TA Q500 TGA instrument. Several single crystals of **1D** (1.1139 mg) were removed from the mother liquor, quickly dried on filter paper to remove surface solvent and placed in a TGA crucible. Measurements were performed under a purified N₂ flow (50 mL/min) by heating at 2.0 °C/min from 30 °C to 300 °C.

TGA on single crystals of form **1D** confirms that methanol molecules are released in the temperature range from 30 °C to 90 °C (Figure S12). The percentage weight loss is 8.2% and corresponds to a methanol content of 1.7 molecules per cyclopeptoid molecule, which agrees with the calculated methanol content according to the X-ray crystal structure (2 methanol molecules per cyclopeptoid molecule).

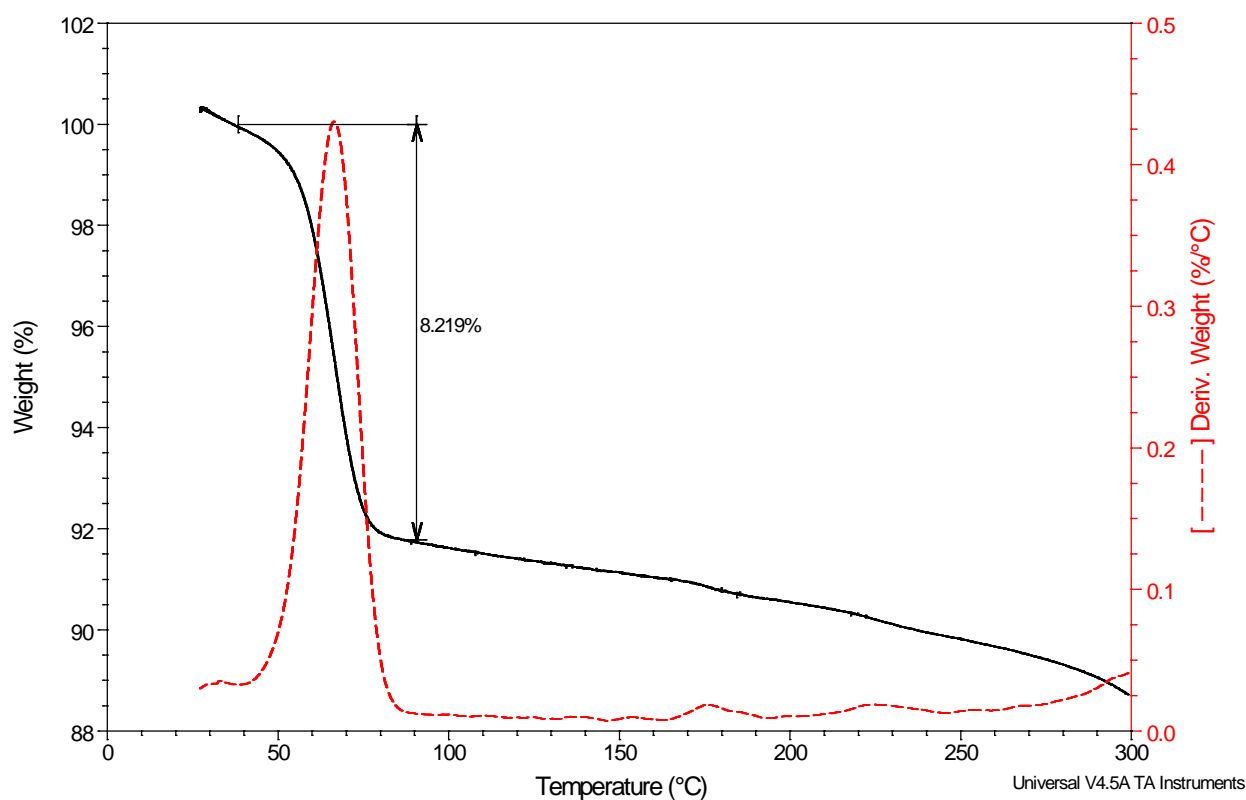


Figure S12. TGA on crystals of form **1D**. Methanol molecules are released in the temperature range from 30 °C to 90 °C.

7. VARIABLE TEMPERATURE X-RAY DIFFRACTION

A crystal of form **1D** (0.35 x 0.35 x 0.15 mm) suitable for laboratory X-ray diffraction was glued on a glass fiber to perform an *in situ* variable temperature experiment. Initially a cell parameter determination was performed at 100 K to confirm that the starting crystal form is **1D**. Then the temperature was raised to 323 K at a rate of 300 K/h and after allowing 20 minutes equilibration time a complete data collection was performed at 323 K. Then, the temperature was raised to 368 K (@ 120 K/h) and after 20 minutes equilibration time a complete data collection was performed at 368 K. Then, the temperature was raised to 393 K (@ 120 K/h) and after 20 minutes equilibration time a unit cell determination was performed. Then the temperature was lowered back to 100 K to allow a full structural determination (@ 120 K/h).

The experiment was performed with MoK α radiation ($\lambda = 0.71073 \text{ \AA}$) using an Oxford Diffraction Excalibur diffractometer equipped with an Oxford 700 Cryostream. Data collection was performed by means of the program CrysAlis CCD.⁴ Data reduction was carried out with the program CrysAlis RED (CrysAlis RED, 2006).⁵ Finally, absorption correction was performed with the program ABSPACK in CrysAlis RED.⁵

The structures were solved by direct methods using the program SIR2014⁶ and refined by means of full matrix least-squares based on F^2 using the program SHELXL.⁷

X-seed⁹ was used as GUI. Non-hydrogen atoms were refined anisotropically. Hydrogen atoms were positioned geometrically and included in structure factors calculations but not refined. Refinement details are summarized in Table S4.

Table S4. Crystallographic data for variable temperature XRD experiments at 100 K, 323 K, 368 K, 393 K and back again to 100 K.

	1D	1F	1F	1F	1F
<i>T</i>	100 K	323 K	368 K	393 K	100 K
Formula	C ₃₀ H ₃₈ N ₆ O ₈ · <i>x</i> CH ₃ OH	C ₃₀ H ₃₈ N ₆ O ₈	C ₃₀ H ₃₈ N ₆ O ₈	C ₃₀ H ₃₈ N ₆ O ₈	C ₃₀ H ₃₈ N ₆ O ₈
Formula weight	667.06	610.66	610.66	610.66	610.66
System	Triclinic	Triclinic	Triclinic	Triclinic	Triclinic
Space group	<i>P</i> -1	<i>P</i> -1	<i>P</i> -1	<i>P</i> -1	<i>P</i> -1
<i>a</i> (Å)	8.5007(14)	8.6467(13)	8.6666(9)	8.708(18)	8.5875(8)
<i>b</i> (Å)	10.3965(11)	10.5283(17)	10.5569(10)	10.58 (2)	10.3508(8)
<i>c</i> (Å)	10.9102(17)	10.6888(18)	10.6926(11)	10.64(2)	10.6762(8)
<i>α</i> (°)	67.863(11)	67.381(16)	67.216(9)	67.17(19)	67.884(7)
<i>β</i> (°)	84.552(15)	87.249(14)	87.313(8)	87.30(17)	86.630(7)
<i>γ</i> (°)	71.048(13)	67.995(15)	67.911(9)	67.72 (19)	68.351(8)
<i>V</i> (Å ³)	844.3(2)	827.5(3)	830.15(16)	830(3)	813.60(13)
<i>Z</i>	1	1	1	1	1
<i>D_x</i> (g cm ⁻³)	1.312	1.225	1.221		1.246
<i>μ</i> (mm ⁻¹)	0.098	0.090	0.090		0.092
<i>F</i> ₀₀₀	356.0	324.0	324.0		324.0
<i>R</i> (<i>I</i> > 2σ <i>I</i>)		0.0552(1305)	0.0741 (1256)		0.0492 (2051)
w <i>R</i> ₂		0.1172(2180)	0.1689(2859)		0.1099 (3081)
N. of param.		199	199		199
Goof		1.023	0.979		1.020
<i>ρ</i> _{min} , <i>ρ</i> _{max} (eÅ ⁻³)		-0.15, 0.12	-0.17, 0.17		-0.21, 0.23

8. REVERSIBILITY TESTS

Form 1C. The stability of form **1C** has also been tested by an *in situ* water vapour exposure SCXRD experiment: a single crystal was inserted into a sealed capillary containing water and analyzed at 296 K by X-ray diffraction. Structure determination still showed the pure form **1C**, even after one week of exposure to water vapours.

Form 1E. A crystal of form **1E** was inserted into a sealed capillary containing methanol and analyzed at 296 K by X-ray diffraction. The structure determination revealed the presence of methanol, thus form **1E** transforms back to form **1D**, demonstrating that the transition from crystal form **1D** to form **1E** is reversible.

REFERENCES

- 1 A. Meli, E. Macedi, F. De Riccardis, V. J. Smith, L. J. Barbour, I. Izzo and C. Tedesco, *Angew. Chem., Int. Ed.*, 2016, **55**, 4679-4682.
- 2 CrystalClear, Crystal Structure Analysis Package, Rigaku-Molecular Structure Corp.
- 3 *APEX Data Reduction Software*, v 6.45; Bruker AXS Inc., Madison, WI, 2003.
- 4 *CrysAlis CCD*, Version 1.171.29.2 (release 20.01. CrysAlis171 . NET); Oxford Diffraction Ltd.: Oxfordshire, U.K., 2006.
- 5 *CrysAlis RED*, Version 1.171.29.2 (release 20.01. CrysAlis171 . NET); Oxford Diffraction Ltd.: Oxfordshire, U.K., 2006.
- 6 M. C. Burla, R. Caliandro, B. Carrozzini, G. L. Casciarano, C. Cuocci, C. Giacovazzo, M. Mallamo, A. Mazzone and G. Polidori, *J. Appl. Cryst.*, 2015, **48**, 306-309.
- 7 G. M. Sheldrick, *Acta Cryst.*, 2015, **C71**, 3-8.
- 8 O. V. Dolomanov, L. J. Bourhis, R. J. Gildea, J. A. K. Howard, H. Puschmann, *J. Appl. Cryst.*, 2009, **42**, 339-341.
- 9 L. J. Barbour, *J. Supramol. Chem.*, 2001, **1**, 189-191.
- 10 C. F. Macrae, I. J. Bruno, J. A. Chisholm, P. R. Edgington, P. McCabe, E. Pidcock, L. Rodriguez-Monge, R. Taylor, J. van de Streek and P. A. Wood, *J. Appl. Crystallogr.*, 2008, **41**, 466-470.
- 11 S. K. Wolff, D. J. Grimwood, J. J. McKinnon, M. J. Turner, D. Jayatilaka and M. A. Spackman, CrystalExplorer (Version 3.1), University of Western Australia, 2013.
- 12 (a) M. A. Spackman and D. Jayatilaka, *CrystEngComm*, 2009, **11**, 19-32; (b) J. J. McKinnon, M. A. Spackman and A. S. Mitchell, *Acta Crystallogr., Sect. B: Struct. Sci.*, 2004, **60**, 627-668;
- 13 M. A. Spackman, *Phys. Scr.*, 2013, **87**, 048103. doi:10.1088/0031-8949/87/04/048103
- 14 J. J. McKinnon, D. Jayatilaka and M. A. Spackman, *Chem. Commun.*, 2007, 3814
- 15 F. H. Allen, O. Kennard, D. G. Watson, L. Brammer, A. G. Orpen and R. Taylor, *International Tables for Crystallography*, ed. A. J. C. Wilson, Kluwer Academic, Dordrecht, 1995, pp. 685-706.
- 16 (a) A. Gavezzotti, *New J. Chem.*, 2011, **35**, 1360-1368; (b) A. Gavezzotti, *J. Phys. Chem. B*, 2003, **107**, 2344-2353; (c) A. Gavezzotti, *J. Phys. Chem. B*, 2002, **106**, 4145-4154.
- 17 M. J. Frisch *et al.*, Gaussian 09, revision A.1; Gaussian, Inc.; Wallingford, CT, 2009.
- 18 S. Grimme, R. Huenerbein and S. Ehrlich, *ChemPhysChem*, 2011, **12**, 1258-1261.